Structural Characterization of the Catalytic High-Spin Heme *b* of Nitric Oxide Reductase: A Resonance Raman Study†

Pierre Moënne-Loccoz*,‡ and Simon de Vries§

Contribution from the Department of Biochemistry and Molecular Biology, Oregon Graduate Institute of Science and Technology, P.O. Box 91000, Portland, Oregon 97291-1000, and Department of Microbiology and Enzymology, Delft University of Technology, Julianalaan 67, 2628 BC Delft, The Netherlands

Received October 23, 1997

Abstract: Nitric oxide reductase (NOR) from *Paracoccus denitrificans* is a transmembrane heterodimer containing a low-spin heme *c*, a low-spin heme *b*, a high-spin heme *b*, and a non-heme iron. Protein sequence similarities between NOR and the cytochrome oxidase superfamily suggest the catalytic center of NO reduction to be the dinuclear high-spin heme *b*/non-heme iron site and the two low-spin hemes to facilitate electron transfer. The EPR-silent character of the non-heme iron and the ferric high-spin heme *b* is believed to be due to an antiferromagnetic coupling between these two metal centers via a bridging ligand. Soret or red excitations on the fully reduced, reduced CO-bound, and fully oxidized states of NOR allow enhancement of the resonance Raman (RR) contributions of the catalytic heme *b* of the enzyme. Resonance Raman spectra of the fully reduced enzyme are consistent with the presence of two six-coordinate low-spin hemes and one five-coordinate heme *b* ligated to a histidine. In the low-frequency region of the RR spectrum, a band at 218 cm^{-1} is assigned to the Fe−N(His) stretching mode of the high-spin heme. Addition of CO induces spectral changes in the high-frequency region of the RR spectra that confirm the binding of CO to the high-spin species. Isotopically labeled CO is used to assign the vibrational modes of the Fe−CO unit: the ν_{Fe-CO} (476 cm^{-1}) and ν_{C-O} (1970 cm^{-1}) as well as the bending mode δ_{Fe-C-O} (569 cm^{-1}). These frequencies show that the catalytic heme is present in an unusual environment, possibly negatively charged, in which CO adopts a geometry quite different from that in cytochrome *c* oxidase (CcO). The RR study of the oxidized enzyme demonstrates that the high-spin heme *b* conserves a pentacoordinate structure in the ferric state. To reconcile the EPR data, which indicate the presence of a bridging ligand in the ferric state of the dinuclear center, with the characteristic five-coordinate RR signature of the high-spin heme *b* in both oxidized and reduced NOR, we propose a mechanism in which the bond between the proximal histidine and the heme iron is broken upon binding of NO, leaving the diiron center bridged after its catalytic turnover.

Introduction

Nitric oxide reductase (NOR) is a cytochrome *bc* complex that reduces NO to N_2O during bacterial denitrification. It is an integral membrane protein, and of all of the enzymes in the denitrification pathway, it is the least well characterized. NOR has been purified by detergent solubilization from different organisms[1−4] and consistently yields an enzyme composed of two subunits, norC, a 16-kDa subunit carrying *c*-type hemes, and norB (54 kDa) which binds *b*-type hemes, but there has been discrepancy regarding the number of redox centers per enzyme. The DNA-predicted amino acid sequences of norB suggest NOR to be a distant member of the superfamily of cytochrome oxidases.[5,6] Similar to subunit I of cytochrome *c* oxidase (CcO), hydropathy plots of norB present 12 potential trans-membrane α-helices. Moreover, the six histidine residues ligating the three crucial cofactors in subunit I of CcO, heme *a* (2), heme a_3 (1), and Cu_B (3), appear to be conserved in norB.[5,7,8] On the basis of these analogies, a stoichiometry of two hemes *b* per heme *c* is expected. Because copper is apparently absent in NOR,[1,7] a putative binuclear metal center equivalent to the heme a_3−Cu_B unit of CcO might contain a non-heme iron instead of Cu.

Recently, a new purification procedure of *Paracoccus denitrificans* NOR using the detergent lauryl maltoside was shown to yield an active enzyme preparation that contains a stoichiometry of two hemes *b*, one heme *c*, and one non-heme iron per enzyme.[4] The electronic absorption spectrum of the oxidized enzyme shows the low-spin *b* and *c* hemes, as well as a broad absorption band at ∼595 nm that is assigned to a high-spin *b* heme. The low-spin *b* and *c* hemes are clearly observed

* To whom correspondence should be addressed. Telephone: 503-690-1673. Fax: 503-690-1464. E-mail: ploccoz@bmb.ogi.edu.

† Abbreviations: CcO, cytochrome *c* oxidase; EPR, electron paramagnetic resonance; 5c and 6c, five coordinate and six coordinate, respectively; HS and LS, high-spin and low-spin electronic configuration of iron, respectively; NOR, nitric oxide reductase; RR, resonance Raman.

‡ Oregon Graduate Institute of Science and Technology.

§ Delft University of Technology.

(1) Heiss, B.; Frunzke, K.; Zumft, W. G. *J. Bacteriol.* **1989**, *171*, 3288−3297.

(2) Kastrau, D. H.; Heiss, B.; Kroneck, P. M.; Zumft, W. G. *Eur. J. Biochem.* **1994**, *222*, 293−303.

(3) Fujiwara, T.; Fukumori, Y. *J. Bacteriol.* **1996**, *178*, 1866−1871.

(4) Girsch, P.; de Vries, S. *Biochim. Biophys. Acta* **1997**, *1318*, 202−216.

(5) Saraste, M.; Castresana, J. *FEBS Lett.* **1994**, *341*, 1−4.

(6) Castresana, J.; Lubben, M.; Saraste, M.; Higgins, D. G. *EMBO J.* **1994**, *13*, 2516−2525.

(7) Zumft, W. G.; Braun, C.; Cuypers, H. *Eur. J. Biochem.* **1994**, *219*, 481−490.

(8) van der Oost, J.; de Boer, A. P.; de Gier, J. W.; Zumft, W. G.; Stouthamer, A. H.; van Spanning, R. J. *FEMS Microbiol. Lett.* **1994**, *121*, 1−9.

S0002-7863(97)03671-8 CCC: $15.00
Published on Web 05/07/1998

in the low-temperature EPR spectrum. The absence of an EPR signal from the high-spin *b* heme and the non-heme iron is interpreted as antiferromagnetic coupling between these two redox centers.[4] Such magnetic coupling is known for the heme a_3-Cu_B unit in CcO[9−10] and in model compounds.[11−13] The reduction of NO is assumed to occur at this redox site whereas the two low-spin hemes *b* and *c* would be involved in electron transfer from soluble cytochrome *c* to the dinuclear center.

Resonance Raman (RR) spectroscopy is a particularly powerful technique extensively used in studies of heme proteins because it selectively probes the vibrational modes of the heme groups and provides structural information on these redox centers.[14] However, its extreme sensitivity to fluorescence of impurities or degradation products resulting from the solubilization of membrane proteins makes this technique strongly dependent on the quality of the purification procedure. In this article, we report the first RR study of NOR, focusing our attention on the high-spin heme *b*. We present RR data on the reduced enzyme as well as its complex with carbon monoxide and draw conclusions about the nature of the proximal ligand and the distal pocket of the catalytic *b* heme. We also demonstrate that, in the fully oxidized enzyme, the high-spin heme is pentacoordinate, a conclusion apparently in conflict with the interpretation of EPR data obtained on the same material. The presence of a five-coordinate high-spin species singles out NOR within the CcO superfamily. A mechanism involving the breaking of the $Fe^{II}-His$ bond upon binding of NO is proposed to account for the pentacoordinate structure of the high-spin species observed in both oxidized and reduced enzyme.

Experimental Procedures

NOR was purified as previously reported and stored under liquid nitrogen.[4] Typical enzyme concentrations for RR experiments were 50−100 μM in a pH 7.0 buffer solution of 20 mM potassium phosphate with 0.05% lauryl maltoside. Reduction to the ferrous state was achieved by addition of microliter aliquots of a 40 mM sodium dithionite solution to an argon-purged sample directly in the Raman capillary cell and was monitored by UV−vis spectroscopy in the same cell.[15] ^{12}CO (CP grade, Air Products) and ^{13}CO (99% ^{13}C, Cambridge Isotope Laboratory) adducts were obtained by injection of 2.5 mL of CO gas through a septum-sealed capillary containing argon-purged, reduced enzyme (∼20 μL).

Resonance Raman spectra were obtained on a McPherson 2061/207 spectrograph (0.67 m) equipped with a Princeton Instruments liquid-N_2-cooled (LN-1100PB) CCD detector. When available for a particular wavelength, Kaiser Optical notch or supernotch filters were used to attenuate Rayleigh scattering. Excitation sources consisted of an Innova 302 krypton laser (406, 413, and 647 nm) and a Liconix 4240NB He/Cd laser (442 nm). The 595-nm excitation wavelength was obtained from an argon-laser pumped dye laser (Coherent Innova 90-6 argon laser, Coherent 599-01 dye laser) using rhodamine 6G (Exciton). Spectra were collected in a 90°-scattering geometry on samples at room temperature with a collection time of a few minutes, whereas longer times and a backscattering geometry were used for low-temperature experiments.[15] Frequencies were calibrated relative to indene and CCl_4 standards and are accurate to ±1 cm^{-1}. CCl_4 was also used to check the polarization conditions. Optical absorption spectra of the Raman samples were obtained on a Perkin-Elmer Lambda 9 spectrophotometer to monitor the samples (fully oxidized, fully reduced, CO complex) both before and after laser illumination.

X-band EPR spectra of the oxidized enzyme were recorded on a Varian E−109 "Century-Series" spectrometer equipped with an Air Products helium cryostat. The EPR spectrometer was operated with experimental conditions similar to those used by Girsch and de Vries[4] and gave an identical spectrum for the oxidized enzyme.

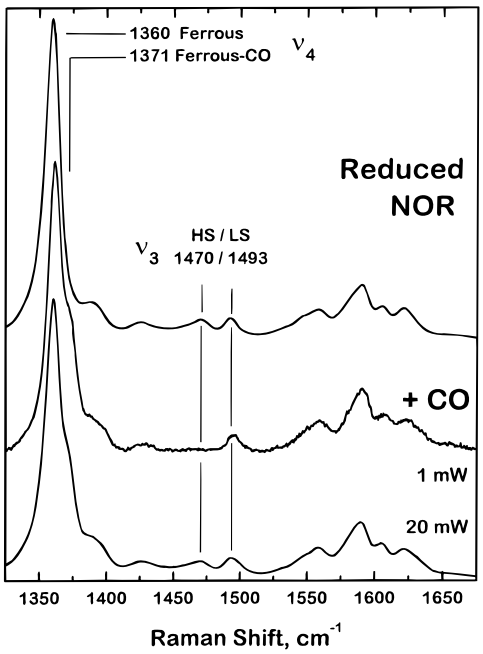

Figure 1. High-frequency region of RR spectra of reduced NOR (top spectrum) and complexed with CO (middle and bottom spectra). Spectra were obtained at room temperature using 413-nm excitation (5 mW for the reduced sample and 1 or 20 mW for the CO complex).

Results and Discussion

Reduced Enzyme and Reduced·CO Enzyme. The high-frequency region of the resonance Raman spectrum of dithionite-reduced NOR obtained with 413-nm excitation is shown in Figure 1 (top trace). RR spectra of metalloporphyrins obtained with Soret excitation are dominated by totally symmetric modes of the porphyrin ring.[14] In reduced NOR, the oxidation-state marker band ν_4 is observed at 1360 cm^{-1}, a frequency characteristic of ferrous hemes. The absence of a shoulder at ∼1372 cm^{-1} confirms the complete reduction of the enzyme. The spin-state marker band ν_3 has two contributions at 1470 and 1493 cm^{-1}, revealing the presence of both high- and low-spin species, respectively (Figure 1, top trace). Because the relative resonance enhancement of the three hemes present in NOR is unknown, one cannot quantitate the high-spin/low-spin (HS/LS) ratio from their respective RR signals. Nonetheless, these data are consistent with a 1/2 ratio of HS/LS hemes.

Upon addition of CO to reduced NOR, the appearance of a high-frequency shoulder on the ν_4 vibration at 1371 cm^{-1}, as well as changes in the ν_3 region with a loss of the 1470-cm^{-1} band of the HS species, indicates CO binding (Figure 1, middle trace). Similar spectral changes are observed in deoxymyoglobin upon binding of CO.[16] The power dependence of the observed RR changes are consistent with the photolabile character of heme-CO complexes. At higher laser power, the

(9) Brudvig, G. W.; Stevens, T. H.; Morse, R. H.; Chan, S. I. *Biochemistry* **1981**, *20*, 3912−3921.
(10) Day, E. P.; Peterson, J.; Sendova, M. S.; Schoonover, J.; Palmer, G. *Biochemistry* **1993**, *32*, 7855−7860.
(11) Holm, R. H. *Pure Appl. Chem.* **1995**, *67*, 217−224.
(12) Karlin, K. D.; Fox, S.; Nanthakumar, A.; Murthy, N. N.; Wei, N.; Obias, H. V.; Martens, C. F. *Pure Appl. Chem.* **1995**, *67*, 289−296.
(13) Martens, C. F.; Murthy, N. N.; Obias, H. V.; Karlin, K. D. *J. Chem. Soc., Chem. Commun.* **1996**, 629−630.
(14) Spiro, T. G.; Li, X. Y. *Resonance Raman Spectroscopy of Metalloporphyrins*; Spiro, T. G., Ed.; John Wiley & Sons: New York, 1988; Vol. 3, pp 1−37.
(15) Loehr, T. M.; Sanders-Loehr, J. *Methods Enzymol.* **1993**, *226*, 431−470.
(16) Tsubaki, M.; Srivastava, R. B.; Yu, N. T. *Biochemistry* **1982**, *21*, 1132−1140.

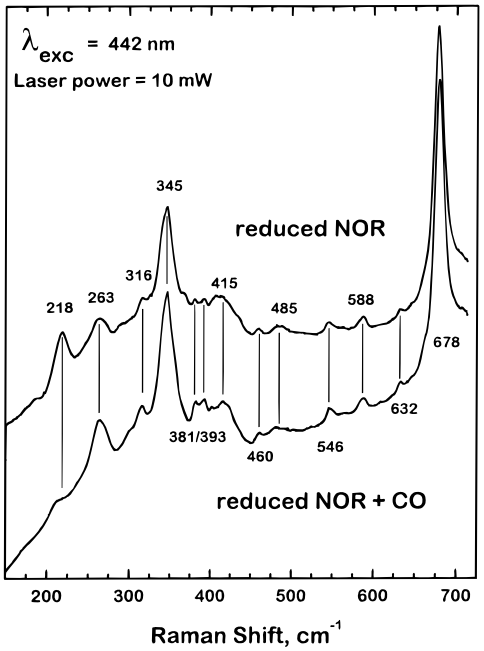

Figure 2. Low-frequency region of the RR spectra of reduced NOR (top spectrum) and complex with CO (bottom spectrum). Spectra were obtained at room temperature using 442-nm excitation (10 mW).

1371-cm^{-1} shoulder characteristic of the Fe^{II}−CO complex diminishes and intensity of ν_3 of the HS species at 1470 cm^{-1} reappears as CO is released (Figure 1, bottom trace). We conclude that CO binds to the HS *b* heme of fully reduced NOR and converts it to a 6cLS species. The low-frequency Fe−CO vibrational modes are discussed in a following section.

Identification of the High-Spin Proximal Ligand. Amino acid sequence homologies between NOR and the superfamily of cytochrome and quinol oxidases predict the presence of a histidine residue as the proximal ligand of the HS heme *b*.[6,8,17] Resonance Raman studies of heme proteins and model compounds have shown that the Fe−N(His) stretching vibration is readily observed between 200 and 250 cm^{-1} in a pentacoordinate ferrous heme with ∼440 nm excitation wavelength, whereas this same vibrational mode is not resonance enhanced in hexacoordinate species.[18] The RR spectrum of reduced NOR excited at 442 nm includes a band at 218 cm^{-1} (Figure 2, top spectrum), a frequency appropriate for $\nu_{Fe-N(His)}$. As expected for the NOR−CO complex where all three hemes adopt a 6cLS state with an inactive iron−histidine stretching mode, no RR bands are observed in the 200−250 cm^{-1} region (Figure 2, bottom spectrum).

In myoglobin, the proximal histidine is only weakly hydrogen bonded and the Fe−N(His) stretch is observed at 221 cm^{-1}.[19,20] Upon hydrogen bonding of the histidine N_δ group, the electron donation of N_ϵ is increased and the Fe−N_ϵ(His) stretching frequency is shifted to higher wavenumbers, as in peroxidases where partial ionization of the proximal histidine yields a $\nu_{Fe-N(His)}$ at ∼245 cm^{-1}.[21,22] The $\nu_{Fe-N(His)}$ frequency of the HS heme of NOR at 218 cm^{-1} implies a coordination of the ferrous HS species to a proximal histidine that is only weakly hydrogen bonded or is not hydrogen bonded, similar to that in CcO, where the Fe−N(His) stretching frequency of heme a_3 has been observed at ∼215 cm^{-1}.[23,24] Our RR data show that, unlike the fungal NOR enzyme which is a member of the cytochrome P-450 superfamily utilizing a thiolate ligated heme and the so-called "push" mechanism,[25] the bacterial version of NOR does not depend on a strong electron donation of the proximal ligand to the catalytic heme. Instead, the observed Fe^{II}−N(His) stretching mode confirms the hypothesis drawn from the alignment of protein sequences in NOR and CcO, showing that the nature and strength of the proximal ligand of their catalytic heme is the same and that their chemical activity depends on a second metal center in the substrate pocket.

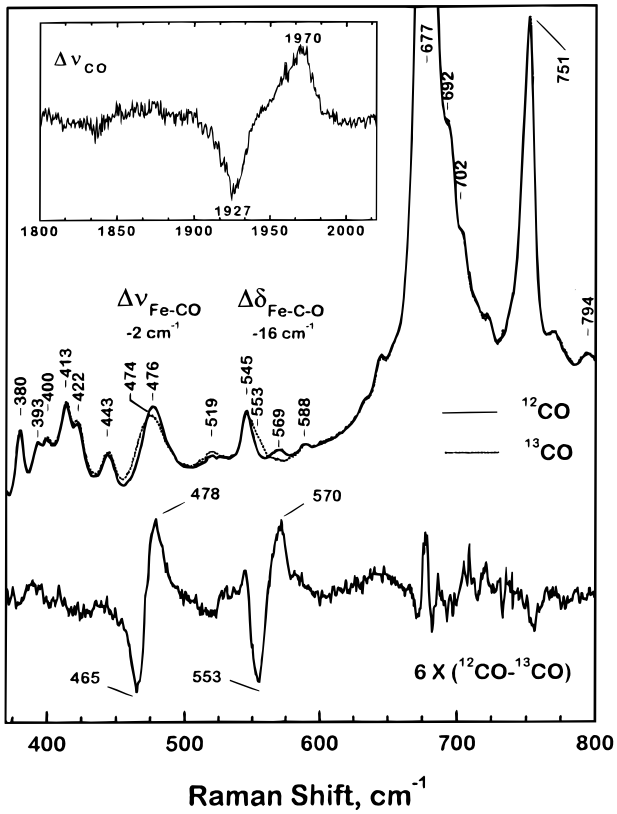

Figure 3. Low-frequency RR spectra of reduced NOR complex with ^{12}CO (solid line) and ^{13}CO (dotted line). The difference spectrum of reduced NOR·^{12}CO complex minus reduced NOR·^{13}CO complex is expanded by a factor of six. The inset shows the same difference spectrum in the high-frequency region. All these spectra were obtained at room temperature using 413-nm excitation (4 mW).

The High-Spin Heme *b* Environment. The Fe−CO vibrational modes of the CO complex of reduced NOR are shown in Figure 3. ^{12}C/^{13}C isotopic substitution allows unambiguous identification of these RR modes. The RR band at 476 cm^{-1} (downshifts 2 cm^{-1} with ^{13}CO) is assigned to the ν_{Fe-CO} stretching mode; the weak band at 569 cm^{-1} (shifts by ∼−15 cm^{-1} upon ^{13}CO substitution) represents the δ_{Fe-C-O} bending mode. The ν_{C-O} stretching mode is also observed in the RR spectrum at 1970 cm^{-1} with a ^{12}C/^{13}C dependency of −44 cm^{-1} (inset to Figure 3). These vibrational frequencies, which differ significantly from typical values found in [FeCO] units of

(17) Saraste, M. *Q. Rev. Biophys.* **1990**, *23*, 331−366.
(18) Kitagawa, T. *Heme protein structure and the iron-histidine stretching mode*; Spiro, T. G., Ed.; John Wiley & Sons: New York, 1988; Vol. 3, pp 97−131.
(19) Kitagawa, T.; Nagai, K.; Tsubaki, M. *FEBS Lett.* **1979**, *104*, 376−378.
(20) Kincaid, J.; Stein, P.; Spiro, T. G. *Proc. Natl. Acad. Sci. U.S.A.* **1979**, *76*, 549−552.
(21) Teraoka, J.; Kitagawa, T. *J. Biol. Chem.* **1981**, *256*, 3969−3977.
(22) Smulevich, G.; Mauro, J. M.; Fishel, L. A.; English, A. M.; Kraut, J.; Spiro, T. G. *Biochemistry* **1988**, *27*, 5477−5485.
(23) Ogura, T.; Hon-nami, K.; Oshima, T.; Yoshikawa, S.; Kitagawa, T. *J. Am. Chem. Soc.* **1983**, *105*, 7781−7783.
(24) Argade, P. V.; Ching, Y. C.; Rouseau, D. L. *Science* **1984**, *225*, 329−331.
(25) Averill, B. A. *Chem. Rev.* **1996**, *96*, 2951−2965.

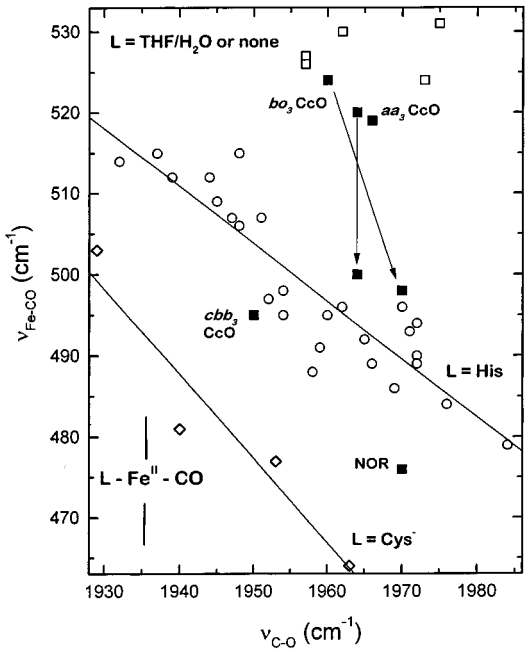

Figure 4. ν_{C-O} vs ν_{Fe-CO} plots of CO complexes of ferrous porphyrins and hemoproteins. The two solid lines correspond to correlations for proximal neutral imidazoles (L = His) as given in ref 27 (open circles), and thiolate-ligated hemoproteins (L = Cys^-), cytochrome P450[27] and NO synthase[49] (open diamonds). Pentacoordinated ferrous porphyrins CO complexes are represented by open squares.[27] The data points for the oxidase superfamily (solid squares) are obtained for the following members: WT and H333A mutant *E. coli bo*$_3$ CcO,[29] bovine *aa*$_3$ CcO[24,50] and WT and H333N *Rhodobacter sphaeroides aa*$_3$ CcO,[28] and *cbb*$_3$-type CcO from *R. capsulatus*.[30] Arrows represent the new coordinates obtained after mutation in the Cu_B site of *R. sphaeroides aa*$_3$ CcO and *E. coli bo*$_3$ CcO.

porphyrin model compounds and other hemoproteins, are sensitive probes of the proximal and distal environments of the heme group,[26,27] and suggest an unusual heme cavity in NOR.

CO is a σ donor as well as a π acceptor. Whereas the iron d_{z^2} orbital is involved in the σ bond, Fe^{II} d_π electrons are donated to the empty π^* orbital of CO. The multiplicity of orbitals involved renders the FeCO vibrational modes sensitive to the nature of both the proximal and distal sides as is shown in Figure 4 where ν_{Fe-CO} and ν_{C-O} frequencies from different heme proteins and model compounds are correlated. Systems with different proximal ligands follow linear correlations that depend on the electron-donating character of the ligand (in Figure 4 from top to bottom: weak or no proximal ligand, imidazole, and thiolate). Fe^{II} $d_\pi \rightarrow$ CO π^* back-bonding is strongly influenced by the polarity of the distal pocket. A positively charged environment and/or hydrogen bonding to the carbonyl will increase back-bonding and will result in a stronger metal−CO bond while weakening the CO bond. Consequently, a linear correlation with a negative slope is observed between ν_{Fe-CO} and ν_{C-O} frequencies (Figure 4). Our RR data obtained on the reduced enzyme have unambiguously characterized the proximal ligand of the HS species as a neutral imidazole of histidine (Figure 2). However, the NOR data point lies below the far end of the histidine-correlation lines, thus indicating an unusual distal pocket environment. The lower end location of NOR in the graph implies that back-bonding is minimized, possibly because of a negatively charged distal pocket. The observation of the bending vibration Fe−C−O at 569 cm^{-1} is also rich in information. Resonance enhancement of this mode can either originate from off-axis distortion or intensity borrowing of the Fe−CO stretching mode via back-bonding interaction.[27] As discussed above, the ν_{Fe-CO} and ν_{C-O} frequencies indicate that back-bonding is weak in the FeCO unit of NOR. Consequently, it is the geometry of the chromophore itself that allows resonance enhancement of the Fe−C−O bending mode. Li and Spiro (1988) have shown that a bent geometry also results in an increase of the energy gap between the stretching and bending frequencies.[26] The 93 cm^{-1} separation between the FeCO stretching and bending modes observed in NOR is significantly larger than the 50−80 cm^{-1} gap observed in most heme proteins, and is fully consistent with a bent geometry for the FeCO unit.

The data points for *bo*$_3$ and *aa*$_3$ CcO are also far off the correlation curve characteristic of hemoproteins ligated to a proximal histidine (Figure 4). This observation was initially proposed to be due to a weak proximal Fe−N(His) bond, but recent investigations combining vibrational spectroscopy and selective mutagenesis have clearly shown that the vibrational frequencies in CcO reflect the properties of the heme distal side and the vicinity of Cu_B rather than the proximal side of the heme.[28,29] In these studies, mutations resulting in a loosely bound Cu_B or a Cu_B-deficient enzyme showed [Fe−CO] vibrations that fell on the correlation curve of histidine ligated hemes (Figure 4). Exactly how the Cu_B site perturbs the CO group bound to heme *a*$_3$ is still unclear. Significantly different interpretations have been proposed ranging from a steric effect of the Cu_B site resulting in a distortion of the Fe−C−O moiety, to a polar interaction of Cu_B on CO leading to a pseudo-bridging Fe−CO−Cu configuration.[28,29] Whereas the CO-complex of CcO is located in the upper part of Figure 4 and NOR at the lower end of the graph, the *cbb*$_3$-type CcO from *Rhodobacter capsulatus*, the type of terminal oxidase most closely related to NOR,[6,8] forms a CO complex whose data point fits reasonably well with the correlation curve.[30] Although more data will be needed to bring a definitive interpretation of these data, some speculations can be made. A tyrosine residue (Y288 *Escherichia coli bo*$_3$ numbering) located in the direct vicinity of the heme *a*$_3$ − Cu_B pocket,[31,32] that is fully conserved in all terminal oxidases binding heme *a*$_3$ or heme *o*$_3$, is replaced by a glycine in *cbb*$_3$ type CcO, and apparently by a glutamic acid in NOR. This glutamate residue may serve as a ligand to the non-heme iron in NOR. Alternatively, this residue might provide a local negative charge yielding the unusual frequencies of the Fe−CO moiety in NOR. In *cbb*$_3$ type CcO, the homologous residue is a glycine, a nonpolar residue leaving the CO complex unperturbed with ν_{Fe-CO} and ν_{C-O} frequencies that fit with the correlation for His-Fe−CO (Figure 4). Another aspect that should be taken into consideration relates to the catalytic reaction of NOR involving two molecules of NO. We cannot presently exclude the possibility that two molecules of CO are bound in the active pocket, one to the HS heme *b* and one to the non-heme iron, resulting in a sterically constrained and electron-

(26) Li, X. Y.; Spiro, T. G. *J. Am. Chem. Soc.* **1988**, *110*, 6024−6033.
(27) Ray, G. B.; Li, X.-Y.; Ibers, J. A.; Sessler, J. L.; Spiro, T. G. *J. Am. Chem. Soc.* **1994**, *116*, 162−176.
(28) Hosler, J. P.; Kim, Y.; Shapleigh, J.; Gennis, R. B.; Alben, J. O.; Ferguson-Miller, S.; Babcock, G. T. *J. Am. Chem. Soc.* **1994**, *116*, 5515−5516.
(29) Uno, T.; Mogi, T.; Tsubaki, M.; Nishimura, Y.; Anraku, Y. *J. Biol. Chem.* **1994**, *269*, 11912−11920.
(30) Wang, J.; Gray, K. A.; Daldal, F.; Rousseau, D. L. *J. Am. Chem. Soc.* **1995**, *117*, 9363−9364.
(31) Iwata, S.; Ostermeier, C.; Ludwig, B.; Michel, H. *Nature* **1995**, *376*, 660−669.
(32) Tsukihara, T.; Aoyama, H.; Yamashita, E.; Tomizaki, T.; Yamaguchi, H.; Shinzawa-Itoh, K.; Nakashima, R.; Yaono, R.; Yoshikawa, S. *Science* **1995**, *269*, 1069−1074.

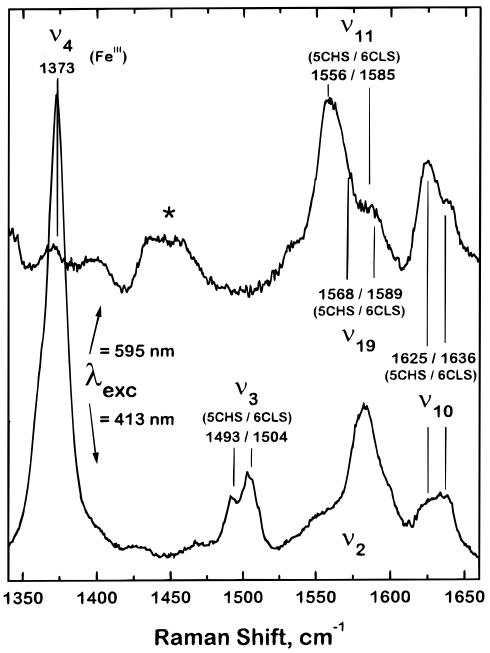

Figure 5. High-frequency region of the RR spectra obtained at room temperature on oxidized NOR with excitation at 413 nm (1 mW) (bottom spectrum) and 595 nm (20 mW) (top spectrum).

rich active site. We are currently investigating this possibility using FTIR spectroscopy.

Oxidized Enzyme. The high-frequency region of the RR spectrum of fully oxidized NOR obtained with 413-nm excitation is shown in Figure 5 (bottom spectrum). The oxidation state marker band ν_4 is observed at 1373 cm^{-1}, a frequency characteristic of ferric heme. The ν_3 and ν_{10} porphyrin skeletal modes are sensitive to the heme core size which varies with the spin and oxidation state of the iron. Typically, for a ferric 6cLS species these two modes are observed at ~1505 and ~1635 cm^{-1}, respectively, and downshift by ~10 cm^{-1} for a 5cHS species and ~20 cm^{-1} for a 6cHS species.[33] In NOR the observed ν_3 and ν_{10} frequencies reveal the presence of 6cLS and 5cHS hemes (Figure 5, bottom spectrum). As previously discussed for the reduced state of the enzyme, we cannot deduce the HS/LS ratio from their respective RR intensities, but again, the 1504 (LS)/1493 (HS) cm^{-1} intensity ratio in the ν_3 region is consistent with the presence of two LS hemes per HS species.

Tuning the excitation wavelength to the 595 nm absorption band is expected to select resonance enhancement of the HS species present in oxidized NOR. Indeed, the spectrum is dominated by contributions from the HS heme, although RR frequencies of the 6cLS hemes are still observed (Figure 5, top spectrum). A depolarized ν_{11} at 1556 cm^{-1}, an inversely polarized ν_{19} at 1568 cm^{-1}, and a depolarized ν_{10} at 1625 cm^{-1} are characteristic of a 5cHS heme and confirm the conclusions drawn from RR data obtained with Soret excitation.

In CcO, the RR signal of the ferric HS species is characteristic of a hexacoordinate heme.[34,35] In addition to its proximal histidine, the HS heme a_3 is believed to coordinate a sixth ligand, possibly a hydroxo group bridging the ferric heme to the Cu_B.[36,37] So far among all the members of the oxidase superfamily studied by RR spectroscopy, only the quinol oxidase of *Sulfolobus acidocaldarius* has been shown to possess a catalytic ferric heme in a penta-/hexacoordination state equilibrium.[38] Our RR results show that the NOR HS heme is at the other extreme of this equilibrium with a pure pentacoordinate structure in its ferric state.

The structural information deduced from the RR spectra obtained on oxidized NOR are in apparent conflict with the conclusions drawn from EPR spectroscopy. Neither the high-spin heme *b* nor the non-heme iron contribute to the EPR spectrum of oxidized NOR, akin to the heme a_3 and Cu_B cluster in cytochrome *c* oxidase. To account for the EPR silence of the HS iron of NOR, Girsch and de Vries[4] proposed an antiferromagnetic coupling via an unidentified bridging ligand. The structure of the HS heme *b* in oxidized NOR would be a His−Fe−O(H) hexacoordinate species, as in CcO. However, our RR experiments clearly display a 5cHS ferric species. The apparent discrepancy between the EPR and the RR data could be due to different experimental conditions. Initially, different temperatures were used in these two experiments, and for this reason, the RR experiments were repeated at 20 K. With red excitation, a fluorescence background already observed at room temperature is greatly amplified at cryogenic temperatures and precluded the acquisition of RR data. However, Soret excitation of the 20 K sample gave a similar result as obtained at room temperature with no evidence of a 6cHS species (data not shown). Although the 5cHS species has been observed with low laser power and low energy photons (less than 0.1 mW at 413 nm and 20 mW at 595 nm), it may be possible that the bridging ligand is extremely photosensitive and thus unobservable by RR spectroscopy. To test this hypothesis the EPR spectrum of NOR has been rerecorded under illumination by a ~300 W continuous white light; however, we observed no spectral changes. Although we cannot rule out the possibility of transient reduction of the enzyme by the laser probe in the RR experiments leading to a different configuration than in the "resting" state studied by EPR, our control experiments strongly suggest that the high-spin heme *b* is pentacoordinate in fully oxidized NOR.

To reconcile the RR and EPR data we propose an alternative to the model put forward previously,[4] and describe the basic reactions involved in the catalytic cycle of NOR (Figure 6). The key feature of this model is that binding of NO to the ferrous HS species results in the dissociation of the proximal histidine. The reduction of 2NO to N_2O leaves the ferric 5cHS heme bridged to the non-heme iron. Upon reduction of the HS heme by electron transfer from the other cofactors, the bridging ligand is lost in favor of the original histidine proximal ligand. Our model is consistent with our RR and EPR observations on the different oxidation states of NOR and it involves mechanisms previously shown to operate in other enzymatic systems. For example, the formation of a pentacoordinate α-NO heme in hemoglobin with dissociation of the proximal histidine is well documented.[39] Similarly, a labile proximal histidine has been characterized in the human NO receptor, soluble guanylyl cyclase. The stable form of the latter enzyme is present as a

(33) Parthasarathi, N.; Hansen, C.; Yamaguchi, S.; Spiro, T. G. *J. Am. Chem. Soc.* **1987**, *109*, 3865−3871.
(34) Babcock, G. T.; Callahan, P. M.; Ondrias, M. R.; Salmeen, I. *Biochemistry* **1981**, *20*, 959−966.
(35) Woodruff, W. H.; Dallinger, R. F.; Antalis, T. M.; Palmer, G. *Biochemistry* **1981**, *20*, 1332−1338.
(36) Fann, Y. C.; Ahmed, I.; Blackburn, N. J.; Boswell, J. S.; Verkhovskaya, M. L.; Hoffman, B. M.; Wikström, M. *Biochemistry* **1995**, *34*, 10245−10255.
(37) Ostermeier, C.; Harrenga, A.; Ermler, U.; Michel, H. *Proc. Natl. Acad. Sci. U.S.A.* **1997**, *94*, 10547−10553.
(38) Gerscher, S.; Dopner, S.; Hildebrandt, P.; Gleissner, M.; Schafer, G. *Biochemistry* **1996**, *35*, 12796−12803.
(39) Hille, R.; Olson, J. S.; Palmer, G. *J. Biol. Chem.* **1979**, *254*, 12110−12120.

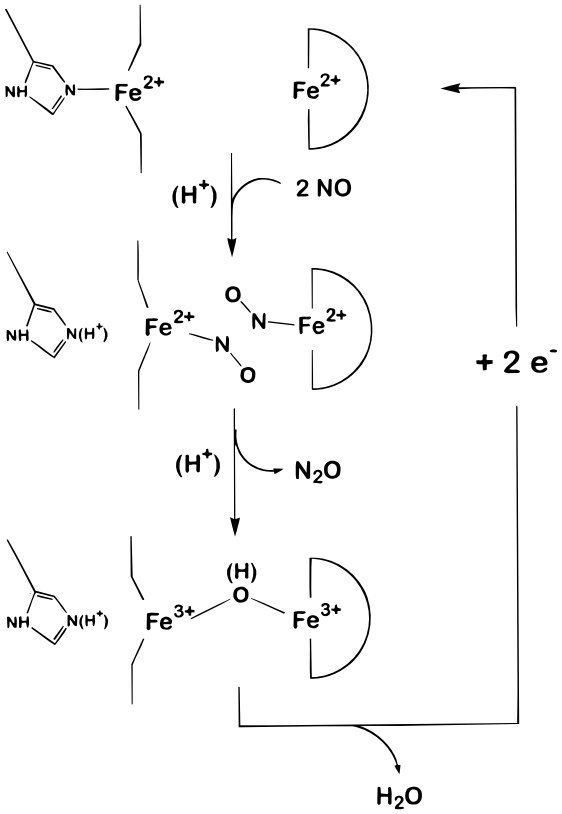

Figure 6. Proposed structures of the catalytic HS heme of NOR and its role during enzyme turnover. The hydrogens within parentheses indicate that the protonation states of the labile proximal histidine and the bridging oxygen atom are unknown.

histidine-ligated 5cHS ferrous heme which, upon binding of NO (but not CO), loses its proximal histidine to form a nitrosyl pentacoordinate species.[40−44] As mentioned earlier, the proximal Fe−His bond strength of the HS heme of NOR is within the range of those of hemoglobin and guanylyl cyclase (GC, 204 cm^{-1}; NOR, 218 cm^{-1}; Hbα, 223 cm^{-1}). Interestingly, the RR studies of the CO complex of soluble guanylyl cyclase reached a similar conclusion to ours, characterizing the distal pocket as a negatively charged environment.[44] The model of Figure 6 bears some resemblance with ligand-exchange mechanisms proposed for CcO to allow strict coupling between electron transfer and proton pumping.[45,46] Woodruff's model[45] described a ligand shuttling between the heme a_3 and Cu_B concomitant with the displacement of heme a_3 proximal ligand, whereas Rousseau's proposal[46] involved a tyrosine side chain located on the proximal side as the replacement ligand. However, recent picosecond time-resolved RR experiments have demonstrated the persistent coordination of the proximal histidine of heme a_3, ruling out ligand-exchange models for CcO;[47] moreover, experimental evidence seems to indicate that NOR is not a proton pump.[48] We are currently conducting further spectroscopic studies on NOR to test our proposed model. In particular, the sensitivity of the HS heme to exogenous ligands should depend on the occupancy of the distal side.

Acknowledgment. We are most grateful to Professor Thomas M. Loehr for helpful discussions, suggestions, and critical reading of the manuscript. P.M.-L. acknowledges financial support for this project under NIH Grant GM 34468 to Thomas M. Loehr. S.D.V. thanks The Netherlands Organization for Scientific Research (NWO) for a travel grant to perform RR experiments at OGI and particularly acknowledges the great hospitality of Professors Thomas M. Loehr and Joann Sanders-Loehr.

JA973671E

(40) Traylor, T. G.; Duprat, A. F.; Sharma, V. S. *J. Am. Chem. Soc.* **1993**, *115*, 810−811.
(41) Yu, A. E.; Hu, S.; Spiro, T. G.; Burstyn, J. N. *J. Am. Chem. Soc.* **1994**, *116*, 4117−4118.
(42) Kharitonov, V. G.; Sharma, V. S.; Pilz, R. B.; Magde, D.; Koesling, D. *Proc. Natl. Acad. Sci. U.S.A.* **1995**, *92*, 2568−2571.
(43) Stone, J. R.; Marletta, M. A. *Biochemistry* **1994**, *33*, 5636−5640.
(44) Deinum, G.; Stone, J. R.; Babcock, G. T.; Marletta, M. A. *Biochemistry* **1996**, *35*, 1540−1547.
(45) Woodruff, W. H. *J. Bioenerg. Biomembr.* **1993**, *25*, 177−188.
(46) Rousseau, D. L.; Ching, Y.; Wang, J. *J. Bioenerg. Biomembr.* **1993**, *25*, 165−176.
(47) Schelvis, J. P. M.; Deinum, G.; Babcock, G. T. *J. Am. Chem. Soc.* **1997**, *119*, 8409−8416.
(48) Shapleigh, J. P.; Payne, W. J. *J. Bacteriol.* **1985**, *163*, 837−840.
(49) Wang, J.; Stuehr, D. J.; Rousseau, D. L. *Biochemistry* **1997**, *36*, 4595−4606.
(50) Yoshikawa, S.; Choc, M. G.; O'Toole, M. C.; Caughey, W. S. *J. Biol. Chem.* **1977**, *252*, 5498−5508.